

Thermal properties and combustibility of cross-linked XNBR/CSM blends

Part I. Influence of the magnesium oxide

G. Janowska · A. Kucharska-Jastrzabek ·
A. Kasiczak · W. M. Rzymiski

Received: 30 June 2010 / Accepted: 10 January 2011 / Published online: 18 February 2011
© Akadémiai Kiadó, Budapest, Hungary 2011

Abstract The article describes the measurement results of the thermal properties of cross-linked blends of carboxylated butadiene-acrylonitrile rubber (XNBR, Krynac X.7.50) and chlorosulfonated polyethylene (CSM, Hypalon 48) under inert gas (DSC, TG) and in air (derivatography). The blends were cross linked at a temperature of 150 °C by means of MgO in the presence of stearic acid. The thermal curves were interpreted from the point of view of phase transitions and chemical reactions of high-molecular components. It has been found that the polymers under investigation show a good compatibility resulting from the presence of both inter-polymeric covalent bonds and inter-polymeric ionic bridges containing magnesium ions that fulfill the role of chemical compatibilizer. The study has shown that XNBR/CSM blends belong to a group of polymeric materials that are self-extinguished in air. Their flammability, determined by OI and the combustion time in air, clearly depends on the cross-linking degree associated with the quantity of MgO incorporated into the blend of elastomers.

Keywords Carboxylated butadiene-acrylonitrile rubber (XNBR) · Chlorosulfonated polyethylene (CSM) · Thermal analysis · Thermal curves (DTA, DSC, TG, DTG) · Combustibility

Introduction

At the Institute of Polymers and Dye Technology of Technical University of Lodz, studies have been carried out for

several years on the inter-elastomeric reactions of cross-linking non-conventional blends of elastomers and the properties of products made in this way. In the blends of carboxylated butadiene-acrylonitrile rubber (XNBR) and chlorosulfonated polyethylene (CSM), one of the components (CSM), due to its low content of reactive functional groups in relation to the cross-linking compound used (MgO, Mg(OH)₂, or other metal compounds), cannot form its own network structure. On the other hand, we have found that the heating of XNBR/CSM blends containing a selected metal compound and stearic acid results in the formation of network structure containing inter-elastomeric cross linkages [1, 2]. The rate and advancement of cross-linking XNBR/CSM blends and the properties of polymeric materials made in this way depend on the blend composition and the type and quantity of metal compound used for cross-linking [3–5].

Currently produced and commercially available CSMs are characterized by different cross-linking capabilities, thermal properties, and flammability [6, 7], which is directly connected with the content of chlorine combined altogether (24–43 wt%) and the content of chlorine combined in chlorosulfonic groups (1.1–1.55 wt%) of these elastomers. Different properties of CSM as a potential flame-retardant compound, dependent on the content of chlorine combined [6, 7], manifest themselves also in different effects of its type and quantity on the thermal properties and flammability of the inter-elastomerically cross-linked blends of CSM and butadiene-styrene (SBR) [8, 9]. The analysis of test results of cross-linked XNBR/CSM and SBR/CSM blends and the thermal properties and flammability of CSM leads to a conclusion that the thermal properties and flammability of XNBR/CSM blends should depend on both the type of CSM incorporated into the blend and the type and quantity of metal compound used for its inter-elastomeric cross-linking. Hence, the aim of this study is to assess the effect of MgO

G. Janowska (✉) · A. Kucharska-Jastrzabek · A. Kasiczak ·
W. M. Rzymiski
Faculty of Chemistry, Institute of Polymers and Dye
Technology, Technical University of Łódź, Łódź, Poland
e-mail: janowska@p.lodz.pl

quantity added to the blend of XNBR and the selected CSM on the thermal properties and flammability of the cross-linking products of such blends. MgO has been used considering its high cross-linking effectiveness confirmed in previous studies [2, 3]. The effect of CSM on the thermal properties and flammability of cross-linked XNBR/CSM blends will be a subject of a separate article.

Experimental

The subject of the present investigations concerned blends [10–32] containing 70 parts by weight of carboxylated butadiene-acrylonitrile rubber (XNBR, Krynac X.7.50, a product from Bayer Lanxess, containing 7% by weight of combined acid and 27.5% by weight of combined acrylonitrile) and 30 parts by weight of chlorosulfonated polyethylene [9, 32] (CSM, Hypalon 48, a product from Du Pont Dow Elastomers, containing 43% by weight of chlorine totally combined, 1.1% by weight of chlorine combined in SO_2Cl groups and 1% by weight of combined sulfur). The XNBR/CSM blends prepared at room temperature by means of a laboratory rolling mill were cross-linked at a temperature of 150 °C using a cross-linking agent including 8, 12, 16, 24, or 32 parts by weight of magnesium oxide (MgO from Ancor-P) in the presence of 2 parts by weight of fatty acid (stearin from POCh) per 100 parts by weight of the elastomer blend. The blends were, respectively, designated with the following symbols: XNBR/CSM-8, XNBR/CSM-12, XNBR/CSM-16, XNBR/CSM-24, and XNBR/CSM-32. The excessive content of MgO in XNBR/CSM-24 and XNBR/CSM-32 blends in relation to the twice as high stoichiometric quantity, in terms of the content of carboxyl groups, fulfills the function of filler in them.

The cross-linking durations of particular XNBR/CSM blends, in the presence of MgO [2, 3, 32] and stearin were consistent in an electrically heated hydraulic press with the values of τ_{90} determined from the results of the cross-linking kinetic measurements obtained by means of a WG-02 vulcameter with an oscillating rotor according to standard PN-ISO 3417: 1994.

The cross-linking degree of XNBR/CSM blends ($\alpha = 1/Q_w$), taking into account both crosswise ionic bonds and crosswise covalent bonds, was determined on the basis of the results of equilibrium swelling (Q_w) in toluene. The cross-linking degree ($\alpha' = 1/Q_{w,a}$), taking into account crosswise covalent bonds was determined from the results of equilibrium swelling ($Q_{w,a}$) in toluene after the action of ammonia vapors.

The measurements of equilibrium swelling were performed also in the case of samples heated in the derivatograph furnace up to appropriate temperatures determined from DTA curves.

The determinations of elasticity constants were carried out with dumbbell samples with a measurement section length of 20 mm and a width of 4 mm. The length of measurement sections before and after loading was determined by means of a cathetometer. The measurement was performed 30 min after each sample loading and the weights were selected so that the sample elongation increment was each time up to 20% of the measurement section length. The measurement was carried out until 120% of the initial measurement section value was obtained. Elasticity constants were determined from Mooney–Rivlin's equation [33, 34].

The mechanical properties [25, 28] of cross-linked XNBR/CSM blends were tested according to standard PN-ISO 37:1998 by means of a Zwick tensile testing machine, model 1435, cooperating with a properly programmed computer. Dumbbells with a measurement section width of 4 mm were used to determine tensile strength (TS_b) and elongation at break (E_b).

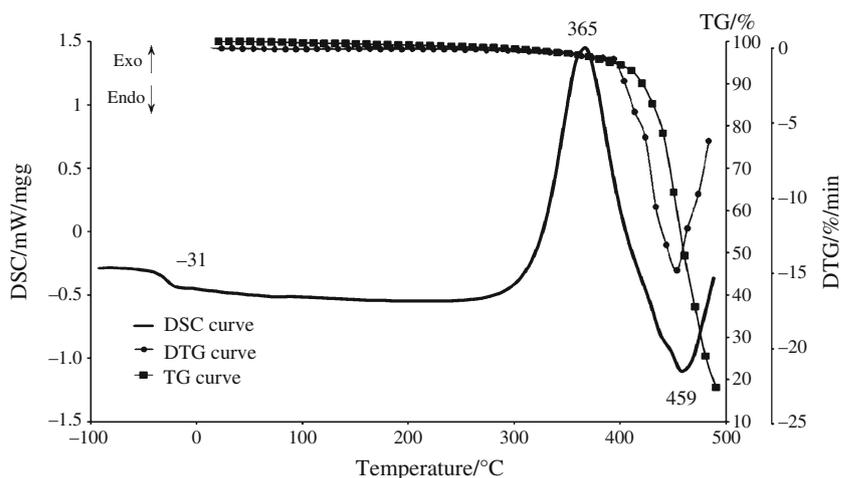
The thermal analysis of cross-linked blends [8–32] was performed under both air and nitrogen atmospheres. 90 mg samples were heated under air in a Paulik, Paulik Erdey derivatograph furnace at a rate of 7.9 °C/min within the temperature range 25–800 °C using Al_2O_3 as a reference substance. Thermal curve sensitivities were as follows: TG = 100, DTA = 1/5, and DTG = 1/20.

Under nitrogen atmosphere [10, 12–18, 20, 25, 28, 30–32], 5–7 mg samples were heated in a DSC-204 furnace from Netzsch at a rate of 10 °C/min within the temperature range from –100 to 500 °C.

The flammability of the cross-linked XNBR/CSM blends was determined by the method of oxygen index using an apparatus of our own construction [35]. The flammability of XNBR/CSM was also assessed on the basis of sample combustion time under air or time, after which the sample was extinguished. The sample shape and dimensions, its arrangement and flame treatment time were the same as in the case of the oxygen index method. It was difficult to make profiled samples for flammability tests due to strong adhesion of elastomers to a metallic mold. The problem was solved thanks to a slight cross-linking of the polymers with the use of dicumyl peroxide or magnesium oxide in the case of XNBR.

The morphology of cross-linked XNBR/CSM blends was examined by means of an atomic force microscope (model: Merology Series 2000, manufacturer: Molecular Imaging USA). Prior to the examinations, samples were cross-linked on a glass in a steal mold for a time resulting from the vulcetric measurements. The glass was washed with acetone to remove impurities and to obtain a proper roughness. Photographs were taken in a contact mode: Cantilever, model CSC, manufacturer: Mikro Masch, Estonia, measurement parameters: resonance frequency 21–38 kHz, force constant 0.30–0.35 N/m, scanning frequency 4 Hz.

Fig. 1 Thermal curves (DSC, TG, and DTG) of XNBR in nitrogen atmosphere



Results and discussion

The transition of XNBR from glassy to elastic state occurs at $T_g = -31$ °C (Fig. 1, Table 1). This rubber maintains its elastic properties up to a temperature of 263 °C, at which its thermal cross-linking begins due to the radical polymerization of butadiene monomeric units [8, 36]. The maximum rate of this process takes place at $T = 365$ °C. One this temperature is exceeded, there begins a slow loss of sample mass indicating that the cross-linking processes of the elastomer under nitrogen are accompanied by the fragmentation of its macromolecules and the formation of volatile decomposition products. After the termination of cross-linking at $T = 414$ °C, there begins a swift destruction resulting in an 85% loss of the initial sample weight (Fig. 1).

Under air, XNBR is cross-linked within two temperature ranges: $\Delta T_1 = 180$ – 260 °C and $\Delta T_2 = 300$ – 350 °C, as indicated by the test results of the equilibrium swelling of the polymer before and after its heating in a derivatograph furnace up to $T = 220$ and 330 °C (Fig. 2). Cross-linking processes within a lower temperature range occur due to

the decomposition of hydroperoxide groups contained in the polymer and formed in it under the influence of heating [37, 38]. Cross-linking processes at ΔT_2 , as under inert gas, take place as a result of the radical polymerization of butadiene monomeric unit. The cross-linking processes in air are accompanied by the thermooxidative destruction resulting in a 5.6% loss of the sample weight. The elastomer cross-linked thermally is rapidly decomposed at $T = 360$ °C. This process initially proceeds with the participation of oxygen—the exothermic peak in DTA curve at $T = 380$ °C. When the rate of the formation of volatile XNBR destruction products exceeds the rate of oxygen

Table 1 Thermal properties of elastomers and their cross-linked blends in nitrogen atmosphere

Thermal parameters	$T_g/^\circ\text{C}$	$\Delta T_C/^\circ\text{C}$	$\Delta H_C/\text{J/g}$	$T_d/^\circ\text{C}$
Sample				
XNBR	-31	263–424	712	459
CSM [7]	10	328–434	398	^a
XNBR/CSM-8	-24	225–410	586	462
XNBR/CSM-12	-23	228–410	590	473
XNBR/CSM-16	-19	237–412	566	478
XNBR/CSM-24	-21	234–419	569	482
XNBR/CSM-32	-20	241–418	528	480

T_g glass transition temperature, ΔT_C temperature range of thermal cross-linking, ΔH_C change of thermal cross-linking enthalpy, T_d temperature of destruction maximum rate

^a Gentle destruction process

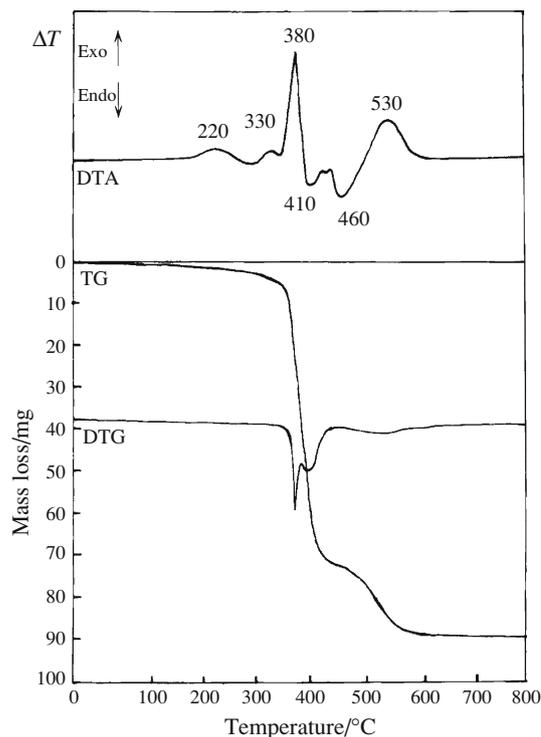


Fig. 2 Thermal curves (DTA, TG, and DTG) of XNBR in air atmosphere

diffusion to the zone of chemical reactions, the elastomer destruction processes become endothermic peaks in DTA curves at $T = 410$ and 460 °C. The symptom of combustion of the solid residue after the thermal decomposition of elastomer, amounting to 19.4% (Table 3), is illustrated by the exothermic transition recorded at $T = 530$ °C (Fig. 2).

The thermal properties of CSMs were the subject of previous studies [6, 7]. The transition of this polymer from the glassy to elastic state occurs at $T_g = 10$ °C (Fig. 6, Table 1). The range of CSM thermal stability is considerably narrower than that of XNBR due to the transitions connected with dehydrochlorination beginning at $T = 190$ °C, that bring about the thermal modification of polymeric chains resulting in the formation of double bonds and conjugate bonds which facilitate thermal cross-linking processes [7].

As a result of heating, CSM in air within the temperature range $\Delta T = 180$ – 300 °C HCl is liberated, and at $\Delta T = 320$ – 380 °C the polymer is thermally cross-linked.

The destruction of thermally cross-linked CSM begins at $T = 390$ °C, while the residue after this process combusts at $T = 500$ °C (Table 3) [6].

From the vulcanometric tests performed, it follows that the increase in MgO incorporated into XNBR/CSM blend does not exert any systematic influence on the optimal time of its vulcanization, τ_{09} , at $T = 150$ °C. With the increase in MgO content, the cross-linking degree of the blend is clearly increased (α , Table 2). The difference $\alpha - \alpha'$ confirms the presence of inter-polymeric ionic bridges containing magnesium ions and performing the function of a chemical compatibilizer. The results of previous studies on XNBR/CSM blends carried out at the Institute of Polymer and Dye Technology of the Technical University of Lodz by the method of IR spectroscopy have shown that one can propose the following mechanism of chemical reactions leading to the formation of cross linkages including inter-elastomeric linkages [1, 2]:

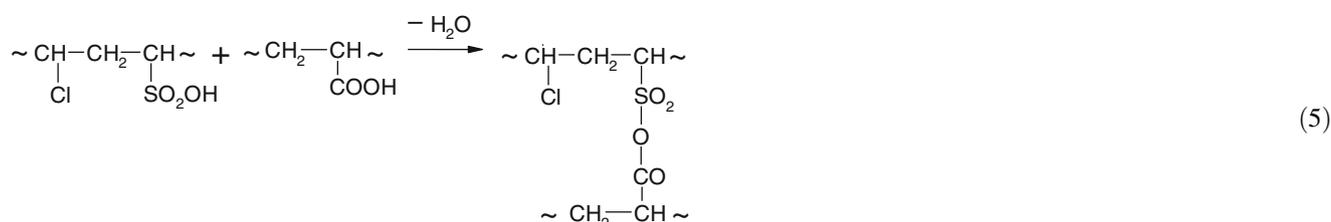
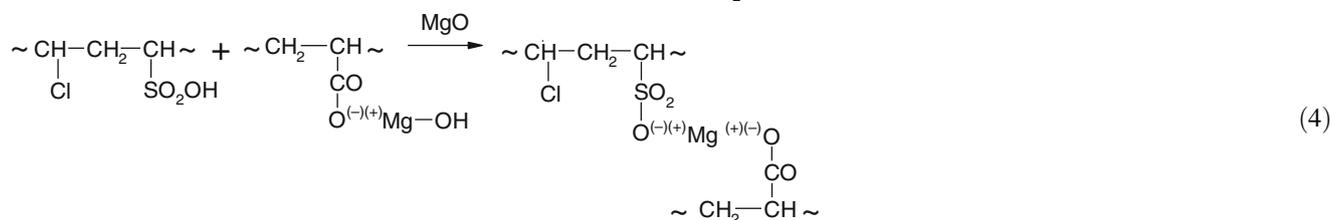
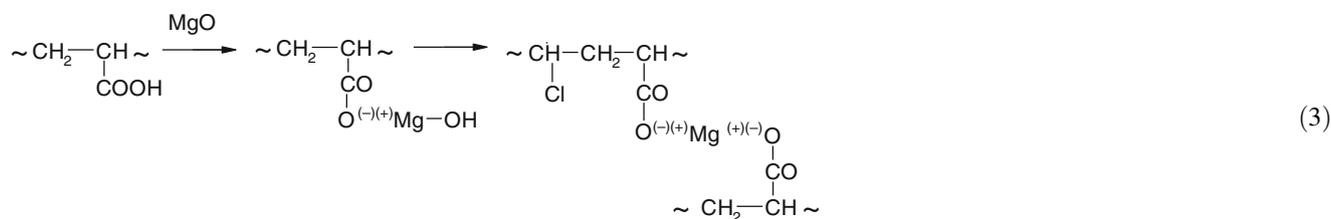
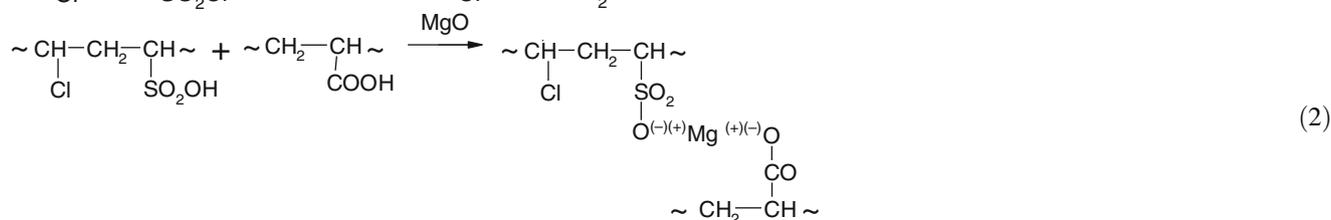
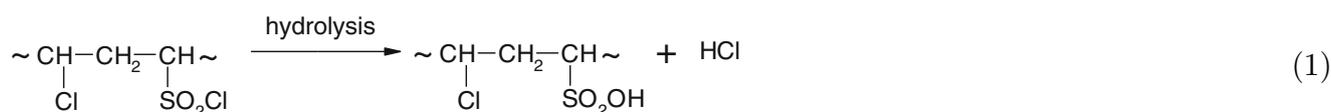


Table 2 Influence of the content of MgO on the crosslinking degree of XNBR/CSM blends and their mechanical properties

Sample	τ_{09}/min	$2C_1/\text{MPa}$	α	α'	$\alpha-\alpha'$	TS_B/MPa	$E_B/\%$
XNBR/CSM-8	44	5.98	0.249	0.228	0.021	28.2	611
XNBR/CSM-12	50	6.31	0.265	0.231	0.034	29.7	591
XNBR/CSM-16	46	7.02	0.293	0.247	0.046	28.3	560
XNBR/CSM-24	53	11.91	0.337	0.321	0.016	27.5	525
XNBR/CSM-32	51	14.25	0.352	0.338	0.014	24.7	483

τ_{09} optimal vulcanization time, $2C_1$ elasticity constant determined from Mooney–Rivlin, α crosslinking degree, taking into account both ionic and covalent crosswise bonds, α' crosslinking degree, taking into account covalent crosswise bonds, $\alpha-\alpha'$ indicator of the content of ionic cross linkages, TS_B tensile strength, E_B elongation at break

Sulfonic groups formed by the hydrolysis of chlorosulfonic groups of CSM under the influence of stearin and the moisture present in the blend (Eq. 1) participate then in co-cross-linking (Eqs. 2, 4, 5) with the carboxylic groups of XNBR to produce inter-polymeric ionic bonds (Eqs. 2, 4) or covalent bonds (Eq. 5). The formation of $-\text{CO}-\text{O}^{(-)(+)}\text{Mg}-\text{OH}$ group (Eq. 3) may be a transient stage leading to their transformation into inter-elastomeric ionic bonds: $-\text{CO}-\text{O}^{(-)(+)}\text{Mg}^{(+)(-)}\text{OSO}_2-$ (Eq. 3).

Test results of the investigation indicate that the increase in the content of MgO in the XNBR/CSM blend increases the degree of its cross-linking resulting from the formation of inter-polymeric covalent bonds (α' , Table 2). From the comparative analysis of the difference $\alpha-\alpha'$, as an indicator of the content of ionic cross linkages, both the intra-elastomeric (XNBR–XNBR) bonds (Eq. 3) and inter-polymeric (XNBR–CSM) bonds (Eq. 4) it follows that their highest content occurs under the influence of cross-linking the XNBR/CSM blend in the presence of 16 parts by weight of MgO/100 parts by weight of the elastomer blend.

The vulcanization of the blends under investigation results in decreased dimensions of MgO particles dispersed in the elastomeric matrix due to their participation in cross-linking processes. In XNBR/CSM-24 and XNBR/CSM-32 blends, the MgO used fulfills also the function of filler as shown by the MgO “island” after their cross-linking (Fig. 3).

The XNBR/CSM blends cross-linked in the presence of MgO and stearin are characterized by good mechanical properties. There is seen a clear effect of the ionic cross linkages on both the values of TS_b and E_b (Table 2).

Similar values of the solubility parameters of XNBR and CSM, amounting to 20.5 and 19.6 MPa [39, 40], respectively, indicate a potential miscibility of these elastomers as confirmed by the results obtained by the DSC method (Table 1). Independently of the quantity of MgO added to XNBR/CSM, the cross-linked blends are characterized by a single temperature of transition from glassy to elastic state, intermediate between T_g values of the high-molecular components of the blend and closer to T_g of XNBR constituting the elastomeric matrix. A slight rise in the glass transition temperature of the blends containing 16, 24, and 32 parts by weight of MgO is due to their increased cross-linking density (Tables 1, 2). The great exothermic transition recorded in the DSC curves of vulcanized XNBR/CSM blends, comprising three peaks at temperatures of 261, 285, and 360 °C, is a symptom of their thermal cross-linking (Figs. 4 and 5). The beginning of this chemical transition, determining the end of the elastic state of vulcanized blends, takes place at $T \geq 225$ °C and clearly shifts toward higher temperatures under the influence of the increasing content of MgO in a sample (Figs. 4, 5). The comparative analysis of enthalpy changes (ΔH_c) leads to a conclusion that the increase in MgO content limits the yield of thermal cross-linking of vulcanized blends, including both intra- and intermolecular chemical reactions

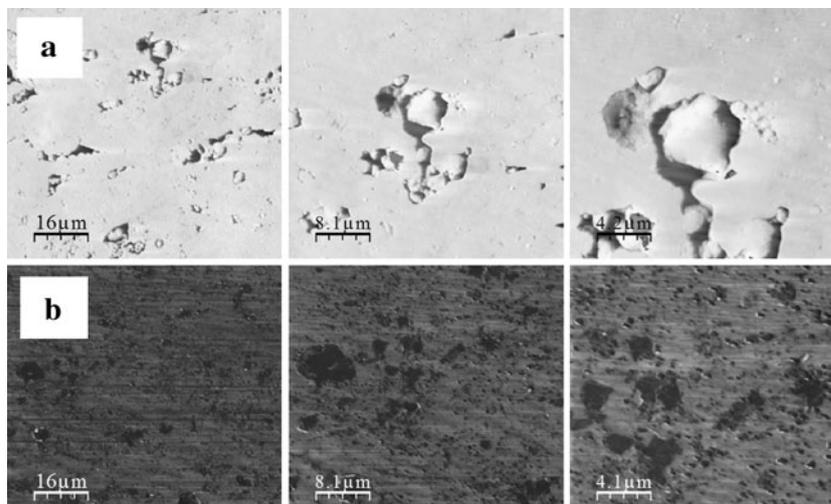
Fig. 3 The morphology of XNBR/CSM-32 blend before (a) and after (b) cross-linking

Fig. 4 Thermal curves (DSC, TG, and DTG) of cross-linked XNBR/CSM-24 blend in nitrogen atmosphere

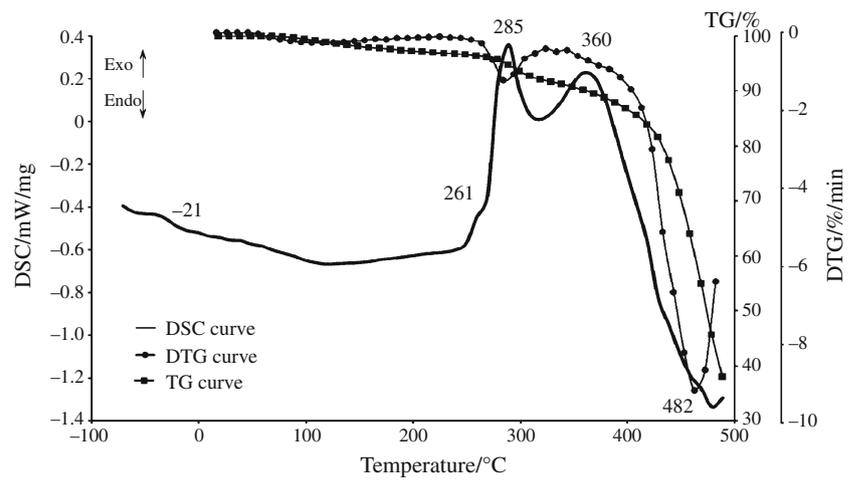


Fig. 5 Thermal curves DSC of cross-linked XNBR/CSM blends in nitrogen atmosphere

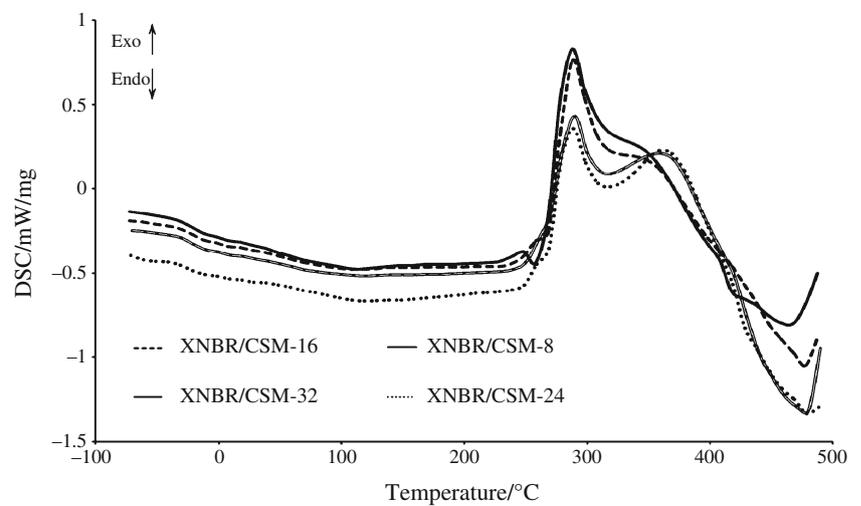
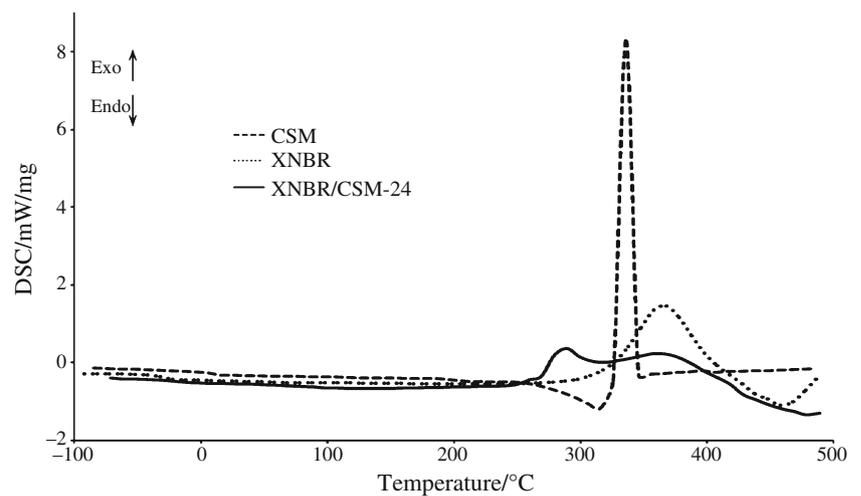


Fig. 6 Thermal curves DSC of XNBR, CSM, and cross-linked XNBR/CSM-24 blend in nitrogen atmosphere



(Figs. 6, 7, Table 1). The thermal cross-linking of the polymeric blends under investigation is accompanied by the destruction of macromolecules and their rapid thermal

decomposition beginning at $T = 427$ °C proceeds slower in comparison with the elastomeric matrix (Fig. 7). The temperature of the maximum destruction rate clearly

Fig. 7 Thermal curves TG of XNBR, CSM, and cross-linked XNBR/CSM-24 blend in nitrogen atmosphere

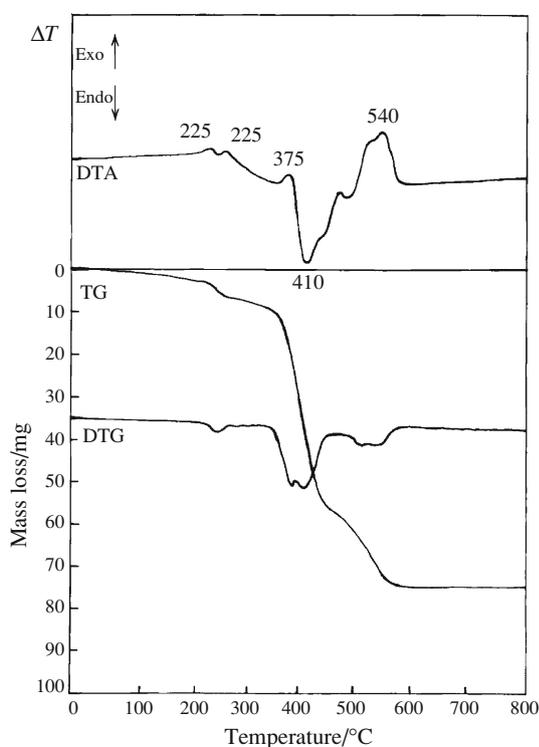
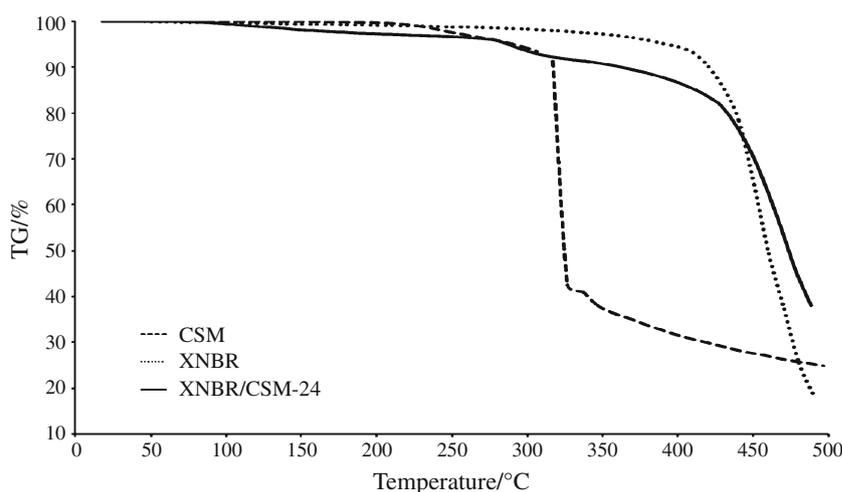


Fig. 8 Thermal curves (DTA, TG, and DTG) of cross-linked XNBR/CSM-24 blend in air atmosphere

increases under the influence of increasing MgO content in the vulcanized elastomeric blends (Table 1).

From the derivatographic analysis of cross-linked XNBR/CSM blends, it follows that they undergo a three-stage decomposition under the influence of heating (TG and DTG curves, Fig. 8). Based on the measurement results of the equilibrium swelling of vulcanized XNBR/CSM before and after heating in a derivatograph furnace up to $T = 225$ and 255 °C, it has been found that the first two exothermic transitions recorded in DTA curves at these temperatures confirm their thermooxidative cross-linking

(Fig. 8). They are accompanied by a considerable loss of sample weight, amounting to 7.8%, due to the liberation of hydrogen chloride combined with CSM (Fig. 8) [6]. The thermal decomposition of XNBR/CSM begins at $T_{D II} \sim 350$ °C and its rate (dm/dt) assumes intermediate values between the decomposition rates of the high-molecular components of the blends. The essential decrease in the destruction rates of the blend tested, in comparison with XNBR matrix, results from the considerable contribution of chemical reactions with an ionic character brought about by the liberating hydrogen chloride (Table 3). This facilitates carbonization processes as indicated by the considerable increase in the residue after the destruction of XNBR/CSM (P_c). The symptom of combustion is illustrated by the great exothermic transition recorded in DTA curve of the blends within the temperature range $\Delta T = 460$ – 545 °C (Fig. 8).

The test results of flammability have shown that the flammability of XNBR does not depend on the cross-linking agent used, mentioned in “Experimental” section (Table 4). XNBR belongs to polymers that extinguish in air, while CSM, whose oxygen index (OI) exceeds 0.375, is a nonflammable polymer as it neither ignites nor glows by means of an external flame source [6]. XNBR/CSM blends tested are self-extinguishing in air and their flammability determined by OI as well as by the burning time in air clearly depends on the cross-linking degree connected with the quantity of MgO incorporated into the blend of elastomers (Tables 2, 4). As the value of OI increases, the length of time, after which the tested sample is extinguished in air, is shortening. The high values of OI and short times, after which the cross-linked blends are extinguished in air, are due to the hydrogen chloride contained in CSM, which is liberated under the influence of elevated temperatures. HCl shows its active action first of all in the flame. As a nonflammable gas, hydrogen chloride decreases the concentration of flammable products in the flame zone and retards

Table 3 Thermal properties of elastomers and their cross-linked blends in air atmosphere

Thermal parameters Sample	$T_5/^\circ\text{C}$	$T_{50}/^\circ\text{C}$	$T_{D\ I}/^\circ\text{C}$	$T_{D\ I\max}/^\circ\text{C}$	$dm/dt\ I/\text{mm}$	$T_{D\ II}/^\circ\text{C}$	$T_{D\ II\max}/^\circ\text{C}$	$dm/dt\ II/\text{mm}$	$P_w/\%$	$P_e/\%$	$T_s/^\circ\text{C}$	$P_{800}/\%$
XNBR	340	415	–	–	–	355 ^a	380	68	–	19.4	530	1.1
CSM [6]	230	375	210	295	26	380	405	30	–	21.1	500	5.5
XNBR/CSM-8	250	415	215	255	6	350	410	40	37.8	35.5	515	10.0
XNBR/CSM-12	245	425	215	250	6	350	405	40	38.9	35.6	500	12.2
XNBR/CSM-16	250	430	220	250	5	350	410	33	38.9	34.6	500	13.9
XNBR/CSM-24	250	430	220	240	5	355	400	32	38.9	32.9	525	17.8
XNBR/CSM-32	260	435	220	260	4	355	415	35	41.4	33.1	525	21.7

T_5 temperature of elastomer/blend 5% mass loss, T_{50} temperature of elastomer/blend 50% mass loss, $T_{D\ I}$ temperature of the first stage of elastomer/blend thermal decomposition, $T_{D\ I\max}$ maximum temperature of the first stage of elastomer/blend thermal decomposition, $dm/dt\ I$ maximum rate of the first stage of elastomer/blend thermal decomposition, $T_{D\ II}$ temperature of the second stage of elastomer/blend thermal decomposition, $T_{D\ II\max}$ maximum temperature of the second stage of elastomer/blend thermal decomposition, $dm/dt\ II$ maximum rate of the second stage of elastomer/blend thermal decomposition, P_e residue after elastomer thermal decomposition, P_w residue after blend thermal decomposition, T_s combustion temperature of residua after elastomer/blend thermal decomposition, P_{800} residue after heating of elastomer/blend up to 800 °C

^a Temperature of XNBR thermal decomposition

Table 4 Combustibility of elastomers and their blends

Sample	t/s	OI
XNBR	129	0.256
CSM [6]	18	>0.375
XNBR/CSM-8	42	0.270
XNBR/CSM-12	27	0.278
XNBR/CSM-16	22	0.298
XNBR/CSM-24	19	0.331
XNBR/CSM-32	16	0.349

t Time after which the tested sample is extinguished in air

OI Oxygen index

the diffusion of oxygen to the flame and inhibits the proceeding chain combustion reactions at the same time. From the derivatographic analysis, it also follows that HCl actively acts also in the combustion zone decreasing the rate of thermal destruction of the cross-linked elastomer blend and facilitates the processes of their carbonization [6, 9]; in this connection a lower quantity of volatile and flammable products of polymer decomposition passes to the flame. In the combustion process, of great importance is also the structure of the boundary layer between the sample (solid phase) and flame (gas phase). In this case, there are formed carbonized elastomers and hence this layer shows a high thermal stability and retards the flow of mass and energy between the solid and gas phases of combustion.

Conclusions

XNBR/CSM blends after cross-linking by means of magnesium oxide are characterized by a single temperature of transition from glassy to elastic state, which indicates a

good compatibility of carboxylated butadiene-acrylonitrile rubber and chlorosulfonated polyethylene resulting from the presence of inter-polymeric covalent bonds as well as inter-polymeric ionic bridges containing magnesium ions that fulfill the function of a chemical compatibilizer.

The thermal decomposition rate of XNBR/CSM assumes intermediate values between the decomposition rates of the high-molecular components of the blend under investigation. The essential decrease in the destruction rate of the blends in comparison with XNBR rubber, constituting the polymeric matrix, results from the considerable contribution of chemical reaction with an ionic character, due to the liberating hydrogen chloride, which facilitates carbonization.

The XNBR/CSM blends under investigation undergo self-extinguishing in air and their flammability determined by OI and the burning time in air, clearly depends on the cross-linking degree associated with the quantity of MgO incorporated into the blends. As the value of OI increases, the length of time, after which the tested sample is extinguished in air, is shortening.

References

- Kozioł M, Rzymiski WM. Curing of blends composed of carboxylated acrylonitrile-butadiene rubber and chlorosulfonated polyethylene. *Ann Pol Chem Soc.* 2004;3:1015–8.
- Kozioł M, Rzymiski WM. Unconventional crosslinking of the blends of chlorosulfonated polyethylene and carboxylated acrylonitrile-butadiene rubber. *Polimery.* 2005;50:587–92.
- Kmiotek M, Rzymiski WM. Interelastomer reactions in unconventional elastomer blends. *Polimery.* 2007;52:511–6.
- Kozioł M, Rzymiski WM, Mackowska A. Effect of type and curing condition on the properties of carboxylated acrylonitrile-butadiene rubber. *e-Polymers.* 2006;P_011:1–6

5. Rzymiski WM, Kmíotek M, Bociąg K. New elastomer on materials made of elastomer blends modified by specific intra- or interelastomer reactions. *Chem Listy*. 2009;103:35–7.
6. Janowska G, Rzymiski WM, Kmíotek M, Kucharska A, Kasiczak A. Thermal properties and combustibility of chlorosulfonated polyethylene. *Polimery*. 2009;54:245–9.
7. Janowska G, Kucharska A, Rzymiski WM, Kasiczak A. DSC study of chlorosulphonated polyethylene. *J Therm Anal Calorim*. 2010;102:1019–24.
8. Janowska G, Kucharska A, Kawalek J, Rzymiski WM. Thermal properties of crosslinked blends of chlorosulfonated polyethylene and styrene-butadiene rubber. *Polimery*. 2009;54:648–53.
9. Janowska G, Kucharska-Jastrzabek A. The effect of chlorosulphonated polyethylene on thermal properties and combustibility of butadiene–styrene rubber. *J Therm Anal Calorim*. 2010;101:1093–9.
10. Radhakrishnan CK, Sujith A, Unnikrishnan G. Thermal behaviour of styrene butadiene rubber/poly(ethylene-co-vinyl acetate) blends TG and DTG analysis. *J Therm Anal Calorim*. 2007;90:191–9.
11. Stankowski M, Kropidłowska A, Gazda M, Haponiuk JT. Properties of polyamide 6 and thermoplastic polyurethane blends containing modified montmorillonites. *J Therm Anal Calorim*. 2008;94:817–23.
12. Lujaji F, Bereczky A, Janosi L, Novak Cs, Mbarawa M. Cetane number and thermal properties of vegetable oil, biodiesel, 1-butanol and diesel blends. *J Therm Anal Calorim*. doi:10.1007/s10973-010-0733-9.
13. Rao V, Johns J. Thermal behaviour of chitosan/natural rubber latex blends TG and DSC analysis. *J Therm Anal Calorim*. 2008;92:801–6.
14. Ying J-R, Liu S-P, Guo F, Zhou X-P, Xie X-L. Non-isothermal crystallization and crystalline structure of PP/POE blends. *J Therm Anal Calorim*. 2008;91:723–31.
15. Rajkumar T, Vijayakumar CT, Sivasamy P, Sreedhar B, Wilkie ChA. Thermal degradation studies on PMMA–HET acid based oligoesters blends. *J Therm Anal Calorim*. 2010;100:651–60.
16. Tan SG, Chow WS. Thermal properties of anhydride-cured bio-based epoxy blends. *J Therm Anal Calorim*. 2010;101:1051–8.
17. Martelli SM, Fernandes EG, Chiellini E. Thermal analysis of soil-buried oxo-biodegradable polyethylene based blends. *J Therm Anal Calorim*. 2009;97:853–8.
18. Chen H, Hu X, Cebe P. Thermal properties and phase transitions in blends of nylon-6 with silk fibroin. *J Therm Anal Calorim*. 2008;93:201–6.
19. Haghghi Yazdi M, Lee-Sullivan P. Determination of dual Glass transition temperatures of a PC/ABS blends using two TMA modes. *J Therm Anal Calorim*. 2009;96:7–14.
20. Kiziltas A, Gardner DJ, Han Y, Yang H-S. Thermal properties of microcrystalline cellulose-filled PET–PTT blend polymer composites. *J Therm Anal Calorim*. doi:10.1007/s10973-010-0894-6.
21. López J, Rico M, Montero B, Díez J, Ramírez C. Polymer blends based on an epoxy-amine thermoset and a thermoplastic. Effect of thermoplastic on cure reaction and thermal stability of the system. *J Therm Anal Calorim*. 2009;95:369–76.
22. Ciesińska W, Zieliński J, Brzozowska T. Thermal treatment of pitch-polymer blends. *J Therm Anal Calorim*. 2009;95:193–6.
23. Afzal AB, Akhtar MJ, Svensson L-G. Thermal studies of DBSA-doped polyaniline/PVC blends by isothermal microcalorimetry. *J Therm Anal Calorim*. 2010;100:1017–25.
24. Kaljuvee T, Rudjak I, Edro E, Trikkel A. Heating rate effect on the thermal behavior of ammonium nitrate and its blends with limestone and dolomite. *J Therm Anal Calorim*. 2009;97:215–21.
25. Rosa DS, Bardi MAG, Machado LDB, Dias DB, Silva LGA, Kodama Y. Starch plasticized with glycerol from biodiesel and polypropylene blends. *J Therm Anal Calorim*. 2010;102:181–6.
26. Menyhárd A, Faludi G, Varga J. β -crystallisation tendency and structure of poly-propylene grafted by maleic anhydride and its blends with isotactic polypropylene. *J Therm Anal Calorim*. 2008;93:937–45.
27. Ciesińska W. Thermorheological studies on polymeric blends. *J Therm Anal Calorim*. 2008;93:747–51.
28. Derval Dos Santos R, Bardi MAG, Machado LDB, Dias DB, Andrade e Silva LG, Kodama Y. Influence of thermoplastic starch plasticized with biodiesel glycerol on thermal properties of pp blends. *J Therm Anal Calorim*. 2009;97:565–70.
29. Dias DS, Crespi MS, Kobelnik M, Ribeiro CA. Calorimetric and SEM studies of PHB–PET polymeric blends. *J Therm Anal Calorim*. 2009;97:581–4.
30. Simoes RD, Rodriguez-Perez MA, de Saja JA, Constantino CJL. Thermomechanical characterization of PVDF and P(VDF-TrFE) blends containing corn starch and natural rubber. *J Therm Anal Calorim*. 2010;99:621–9.
31. Perez CJ, Vázquez A, Alvarez VA. Isothermal crystallization of layered silicate/starch-polycaprolactone blend nanocomposites. *J Therm Anal Calorim*. 2008;91:749–57.
32. Markovic G, Marinovic-Cincovic M, Vodnik V, Radovanovic B, Budinski-Simendic J, Veljkovic O. Thermal stability of acrylonitrile/chlorosulphonated polyethylene rubber blend. *J Therm Anal Calorim*. 2009;97:999–1006.
33. Mooney M. A theory of large elastic deformation. *J Appl Phys*. 1940;11:582–92.
34. Rivlin RS. Torsion of a rubber cylinder. *J Appl Phys*. 1947;18:444–9.
35. Patent PRL 129411 (1987).
36. Janowska G, Kucharska A. The influence of the method of butadiene rubbers cross-linking on their thermal properties. *J Therm Anal Calorim*. 2009;96:561–5.
37. Slusarski L, Janowska G. Thermal decomposition of homo- and copolymers of isobutylene. *J Therm Anal Calorim*. 1980;19:435–47.
38. Janowska G, Slusarski L. Thermal properties of cis-1,4-poly(butadiene). *J Therm Anal Calorim*. 2001;65:205–12.
39. Rzymiski WM, Srogosz A. The solubility parameter of chlorosulfonated polyethylene. *Polimery*. 2000;45:41–5.
40. Rzymiski WM, Koziol M. Kohäsionseigenschaften von karboxylierten Nitrilkautschuken. *Polymerwerkstoffe* 2006. Halle/Saale 27-29.09.2006, p. 196.